

UC Irvine

UC Irvine Previously Published Works

Title

Cerebrovascular phenotypes in mouse models of Alzheimer's disease

Permalink

<https://escholarship.org/uc/item/48g3d8cj>

Journal

Cerebrovascular and Brain Metabolism Reviews, 41(8)

ISSN

1040-8827

Authors

Szu, Jenny I
Obenaus, André

Publication Date

2021-08-01

DOI

10.1177/0271678x21992462

Peer reviewed



Cerebrovascular phenotypes in mouse models of Alzheimer's disease

Jenny I Szu¹ and André Obenaus² 

Abstract

Alzheimer's disease (AD) is a devastating neurological degenerative disorder and is the most common cause of dementia in the elderly. Clinically, AD manifests with memory and cognitive decline associated with deposition of hallmark amyloid beta (A β) plaques and neurofibrillary tangles (NFTs). Although the mechanisms underlying AD remains unclear, two hypotheses have been proposed. The established amyloid hypothesis states that A β accumulation is the basis of AD and leads to formation of NFTs. In contrast, the two-hit vascular hypothesis suggests that early vascular damage leads to increased accumulation of A β deposits in the brain. Multiple studies have reported significant morphological changes of the cerebrovasculature which can result in severe functional deficits. In this review, we delve into known structural and functional vascular alterations in various mouse models of AD and the cellular and molecular constituents that influence these changes to further disease progression. Many studies shed light on the direct impact of A β on the cerebrovasculature and how it is disrupted during the progression of AD. However, more research directed towards an improved understanding of how the cerebrovasculature is modified over the time course of AD is needed prior to developing future interventional strategies.

Keywords

Alzheimer's disease, cerebrovascular, amyloid beta, cerebral amyloid angiopathy, transgenic mice

Received 28 September 2020; Revised 16 December 2020; Accepted 6 January 2021

Introduction

Alzheimer's disease (AD) is a progressive degenerative disorder and is the most common cause of dementia in the elderly.¹ Clinically, AD manifests with memory and cognitive deficits alongside changes in mood and behavior,² which diminish a person's ability to perform everyday tasks.¹ There are two main types of AD: 1) sporadic with a late onset (LOAD), which is observed in ~95% of AD cases, and 2) familial with an early onset (familial Alzheimer's disease; FAD), which is seen in ~5% of AD cases.² Cardinal pathological features of AD include aggregation of extracellular senile plaques composed of amyloid- β (A β) peptide³ and intracellular neurofibrillary tangles (NFTs) consisting of accumulation of filamentous hyperphosphorylated tau protein.⁴ In brief, A β is generated from sequential proteolytic cleavage of its large amyloid precursor protein (APP) where β -amyloid cleaving enzyme (BACE) produces a C-terminal APP fragment that is subsequently cleaved by γ -secretase. This sequence of events ultimately leads to the release

of various isoforms of A β peptides with A β ₄₀ and A β ₄₂ being the most common.⁵ Abnormal regulation of kinases and phosphatases are thought to contribute to formation of NFTs which are comprised of paired helical filaments (PHFs) and straight filaments of hyperphosphorylated tau.⁶

Although the pathogenesis of AD remains stubbornly unclear, two hypotheses have been proposed. The amyloid hypothesis states that accumulation of A β is not only the main cause of AD pathology but that it leads to formation of NFTs, impaired vasculature, and

¹Institute for Memory Impairments and Neurological Disorders, University of California Irvine, Irvine, CA, USA

²Department of Pediatrics, University of California Irvine, Irvine, CA, USA

Corresponding author:

André Obenaus, Department of Pediatrics, School of Medicine, University of California Irvine, Hewitt Hall, Rm 2066, Irvine, CA 92697-4475, USA.

Email: obenaus@uci.edu

cell loss.⁷ For example, mice overexpressing both APP and tau exhibited increased NFTs compared with mutant mice expressing tau protein alone, suggesting that accumulation of A β impacts formation of NFTs.⁸ Additionally, genetic variability in APP processing has also been linked to increased risk of LOAD.⁷ Currently, the apolipoprotein E (*APOE*) gene is the only known genetic risk factor for LOAD⁹ and genetic variability on the low-density lipoprotein receptor-related protein (LRP) gene has demonstrated that LRP may be involved in the pathogenesis of AD.¹⁰ While the amyloid hypothesis is strongly supported, findings challenging it have also emerged. Most notably, a lack of correlation between amyloid burden and the degree of cognitive decline has yet to be determined.¹¹ Moreover, NFTs were observed in autopsied human brains devoid of amyloid.¹²

A reconsideration of the amyloid hypothesis has been recently proposed.¹³ The alternative two-hit vascular hypothesis suggests that vascular damage (hit 1) can result in increased accumulation of A β deposits in the brain (hit 2).¹⁴ While aging remains the most critical risk factor of AD, mounting evidence suggests that vascular pathology is involved in the development of AD, and thereby in support of the vascular hypothesis. Multiple epidemiological and clinical studies have examined vascular risk factors including cardiovascular disease, hypertension, hyperlipidemia, diabetes mellitus, and atherosclerosis attributing to the development of AD.¹⁵ Early studies showed that chronic cerebrovascular insufficiency in young and aged rats not only led to reduced cerebral blood flow (CBF) but also impaired spatial memory dysfunction and hippocampal neuronal damage,¹⁶ deficits observed in human AD pathology.¹⁷ A correlation between traumatic brain injury (TBI) and AD is also well-recognized.^{18,19} In particular A β plaques have been observed within hours following a head injury^{20,21} which can persist years later¹⁹ thereby accelerating the risk of developing AD.

While most of the AD research has focused primarily on neuronal and glial dysfunction, compelling data are emerging identifying a significant vascular component during disease progression. For example, individuals with early cognitive dysfunction exhibited brain capillary damage and compromised blood-brain barrier (BBB) independent of A β and tau.²² Patients with mild cognitive impairments (MCI) also exhibit various vascular derangements, including impaired cerebral hemodynamics, and have an increased probability of developing AD.²³ In the 3xTg AD mouse model, early reductions in brain vascular volume precede the presence of AD hallmark lesions.²⁴ These studies and others suggest that early vascular dysfunction may be a significant driver in AD pathology. Unfortunately, at

present the role of the cerebrovasculature in AD is poorly understood both in clinical populations and in preclinical AD models.

Given the known vascular dysfunction and its association with AD, the architecture of the cerebrovasculature has been relatively unexplored in preclinical models of AD. In this review, we begin by highlighting the structural and functional vascular modifications observed in mouse models of AD, primarily focusing on mouse lines that overexpress APP. This is followed by a discussion on mechanisms of vascular A β clearance and how impairments in these pathways may contribute to AD. Next, we describe the functional role of the neurovascular unit (NVU), specifically focusing on pericytes, astrocytes, and neurons to examine how a compromised NVU potentially contributes to the observed cerebrovascular phenotypes in AD. We conclude by discussing putative cerebrovascular directed therapies that may mitigate or prevent the progression of AD.

Cerebral amyloid angiopathy in transgenic mouse models of AD

Increasing evidence suggests a critical role of cerebrovascular dysfunction in the development and progression of AD.²⁵ Early accumulation of vascular A β not only impairs cerebrovascular function but contributes to cerebral amyloid angiopathy (CAA), a common feature of AD, which has been shown to affect an astounding 80–90% of AD cases.²⁶ Recently, two types of sporadic CAA have been identified. Type 1 CAA is characterized by the presence of A β in cortical capillaries, leptomeningeal and cortical arteries, arterioles, veins, and venules, whereas Type 2 is characterized by A β in the leptomeningeal and cortical vessels only.²⁷ In rodent models of AD, CAA deposits were found between vascular smooth muscle cells (VSMCs) in a banding^{28,29} or ring³⁰ pattern. The banding of CAA increased over time with increasing CAA severity and age suggesting new A β deposits and expansion of existing A β deposits.^{28,29} Similarly, in autopsied human AD brains, A β deposition in the leptomeningeal arterioles form discrete banding patterns that was associated with the VSMCs.³¹ Although CAA can occur independent of AD, the incidence and severity of CAA was increased in AD and correlated with A β plaques and NFTs.³²

Despite considerable research effort, the vascular pathophysiology of AD remains unclear. To identify the mechanisms underlying AD and the development of successful treatments requires preclinical animal models that recapitulate human AD. Over the past few years, the generation of transgenic mouse lines

with elements of AD-like pathology have been instrumental in identifying potential pathways to AD.³³ Studies utilizing animal models that develop CAA or vascular amyloid deposits can assist in identifying mechanisms underlying AD. The most common mouse lines generated are those overexpressing APP with over 50 transgenic mouse lines.³⁴ Below, we describe known transgenic mouse models of AD that have been reported to exhibit marked morphological and functional vascular impairments, as summarized in Table 1 and Figure 1.

Vascular abnormalities of transgenic mouse models overexpressing APP

PDAPP

The PDAPP mice were developed by using a platelet derived growth factor- β (PDGF- β) promoter to drive human APP transgene encoding the FAD APP717 mutation. These mice exhibit age-dependent A β deposits in the hippocampus, corpus callosum, and cortex, which were found to be surrounded by reactive astrocytes. Additionally, PDAPP mice displayed dystrophic neuritic components, gliosis, and reductions in synaptic density.³⁵ Structurally, the vessels of 9 mo old PDAPP mice exhibited significantly increased VSMC wall thickness compared to WT mice, indicative of hypertrophy and/or hyperplasia. Amyloid deposits were consistently found situated next to degenerative vessels, particularly around and within the VSMC layers.³⁶ Interestingly, whole brain multiphoton imaging did not reveal widespread CAA in 22–24 mo old PDAPP mice.²⁸

Tg2576. The Tg2576 strain is one of the most widely used mouse models of AD. It was developed by overexpressing human APP695 with a double Swedish mutation (K670N/M671L) under the control of hamster prion protein promoter (PrP). These mice develop significant parenchymal A β by 11–13 mo of age. Learning and memory is normal at 3 mo of age, however, declines by 9–10 mo of age.³⁷ Using various ages of Tg2576 mice (10 to >22 mo old), three consistent stages of CAA progression were identified. In the “limited” stage, CAA can be observed in the anterior and middle cerebral arteries. In the “intermediate” stage, the presence of CAA can be found in smaller vessels in the anterior half of the dorsal surface. Finally, in the “wide-spread” stage, extensive CAA can be seen in almost all vessels on the dorsal surface spreading towards the ventral surface.²⁸ Compared to control mice, quantification of PECAM-1 for brain capillary vessels revealed an ~30% decrease in vascular density in the cortex and hippocampus of 9 and 17 mo

old male Tg2576 mice, respectively.³⁸ In the corpus callosum, 10 mo old male Tg2576 mice exhibited a marked decrease in the capillary total length, volume, and surface area compared with age-matched controls.³⁹

Cerebrovascular dysfunction was also observed in 19 mo old Tg2576 mice. CBF was significantly reduced in 19 mo old Tg2576 mice compared to age-matched controls and in 8 mo old Tg2576 mice after hypercapnic challenge and whisker stimulation. Moreover, the vasoconstrictive response was measured by inducing cortical spreading depression by occluding the distal middle cerebral artery.⁴⁰ Cortical spreading depression causes an initial transient hypoperfusion followed by a prolonged post-cortical spreading depression oligemia.⁴¹ The initial hypoperfusion and post-cortical spreading depression oligemia were diminished in 19 mo old Tg2576 mice compared to age-matched controls and 8 mo old Tg2576 mice. Finally, the vasodilatory response was tested by measuring resting CBF using isoflurane and α -chloralalose. An increase in resting CBF is generally observed under normal conditions, however a decrement in resting CBF was observed in 19 mo old transgenic mice that was not present in 8 mo old Tg2576 mice or control mice under these conditions.⁴⁰ This suggests that the presence of vascular amyloid contributes to impairments in vasoconstriction and vasodilation. Indeed, 19 mo old Tg2576 mice exhibited severe vascular A β deposits whereas 8 mo old Tg2576 mice have virtually no A β in the vasculature despite the presence of parenchymal A β .⁴⁰

APP23

The APP23 transgenic mouse line overexpresses human APP751 containing the Swedish (K670N/M671L) and London V717I mutations. These mice display extensive amyloid pathology and increased hyperphosphorylated tau protein as early as 6 mo of age.⁴² Spatial memory deficits, which worsen with aging, have also been reported.⁴³ Despite being a widely used model of AD, only a handful of studies have reported altered cerebrovasculature in these mice.

Using vascular corrosion casts and scanning electron microscopy (SEM),⁴⁴ the 3D cerebrovascular architecture of 7–27 mo old APP23 and WT mice were characterized.^{45–49} In WT mice vascular casts displayed a dense capillary network where arteries and veins were distinguishable by imprints of either elongated or rounded endothelial cells (ECs), respectively.⁴⁶ In contrast, APP23 mice displayed a multitude of vascular malformations including swelling, looping, twisting, and kinking, similar to vascular alterations present in the human AD brains.^{47,50–52} Functionally, flow patterns in WT mice were normal as measured by magnetic resonance angiography (MRA), but in APP23 mice

Table 1. Summary of cerebrovascular phenotypes in mouse models of AD.

Strain	Sex	Age	Cerebrovascular phenotype	References
PDAPP	n/a	10–26 mo	<ul style="list-style-type: none"> Significant but not extensive CAA by 22 mo Vessels have significantly increased smooth muscle thickness indicative of hypertrophy and/or hyperplasia Amyloid deposits consistently found next to degenerative vessels 	Domnitz et al. ²⁸
	n/a	9 mo		Zago et al. ³⁶
Tg2576	n/a	10–26 mo	<ul style="list-style-type: none"> Significant decrease in vascular density in the hippocampus compared to cortex Significant decrease in cortical vascular density at 9 and 17 mo Significant decrease in hippocampal density at 17 mo 	Paris et al. ³⁸
		2d, 12 mo, 20 mo		<ul style="list-style-type: none"> Widespread thioflavin-s staining in pial arterioles at 19 mo No vascular amyloid deposits at 8 mo Attenuated resting CBF at 19 mo Significant CBF reductions during hypercapnic challenge and whisker stimulation at 19 mo Attenuated CBF at 19 mo
	n/a	8 and 19 mo	<ul style="list-style-type: none"> Age-dependent progressive accumulation of CAA Marked decrease in length, volume, and surface area of capillaries in the corpus callosum 	
	n/a	10–26 mo 10 mo		Zhang et al. ³⁹
APP23	Both	3–27 mo	<ul style="list-style-type: none"> Vessels exhibited deformations such as swelling, kinking, twisting, and looping Holes and microvascular density are increased in late-stage AD 	Beckmann et al., ⁴⁵
				Heinzer et al., ⁴⁸ Heinzer et al., ⁴⁹ , Meyer et al., ⁴⁶ Krucker et al. ⁴⁷
APP/PS1	M	7 mo	<ul style="list-style-type: none"> Significant reduction in capillary segments Significant increase in BBB permeability at 14 and 24 mo Compromised BBB in CA1 with loose tight junctions Vessels appear bended and tangled and thicker basement membrane contained transparent bubble-like structures Non-uniform vessel diameters Capillaries exhibited microaneurysms within individual segments and spanning bifurcations Numerous protrusions on discrete sections of capillary walls Thinner, disorganized, and less uniform vessels Significant reductions of hippocampal vessel diameter and volume Increased branching pattern with greater distal fine branches Significant reductions in branched angles Vascular lumen appear rugged with irregular lumen at new branch openings 	Lee et al. ⁶⁰
	Both	24 mo		Minogue et al. ⁶³
	n/a	12 mo		Wang et al. ⁶²
	M	9 mo		Kelly et al. ^{57,58}
M	24 mo	Zhang et al. ³⁹		
5XFAD	F	8 mo	<ul style="list-style-type: none"> Disconnected short length capillaries near amyloid deposits Significantly shorter tight junctions Progressive CAA on leptomeningeal and penetrating vessels as early as 3 mo Sporadic perivascular amyloid accumulations on 	Kook et al. ⁷⁰
	F	2–12 mo		Giannoni et al. ⁶⁸
	F	4.5 and 9 mo		

(continued)

Table 1. Continued.

Strain	Sex	Age	Cerebrovascular phenotype	References
			parenchymal microvessels	
			<ul style="list-style-type: none"> • Parenchymal microvascular damage parallels plaque formation starting in fronto-parietal cortices and later into hippocampus • Microvascular leakage appearing at 4 mo • Reduction in microvascular length as early as 2 and 4 mo • Decrease vessels and deteriorated vessels • Vessels associated with $A\beta$ plaques appear fuzzy and distorted • Decrease in tight junction protein ZO-1 • Significant reduction in brain vessels of 9 mo mice • Increased vascular $A\beta_{40}$ and $A\beta_{42}$ with age • Progressive CAA with age • Increased arteriolar tortuosity and curvature and smaller arteriolar radius 	Ahn et al. ⁶⁹ Dorr et al. ³⁰
TgCNRD8	n/a	2–12 mo		
Tg-SwDI	n/a n/a	3–12 mo	<ul style="list-style-type: none"> • Early-onset and robust accumulation of $A\beta$ in isolated microvessels • Significant increases in $A\beta_{40}$ and $A\beta_{42}$ in isolated microvessels as early as 3 mo • Apparent microhemorrhage on microvessels next to $A\beta$ deposits • Accumulation of fibrillary amyloid in microvessels at 3 mo 	Davis et al. ⁷⁷
		3 and 6 mo		
APPDutch	n/a	Variable	<ul style="list-style-type: none"> • CAA highest in subiculum • CAA appears at ~22–25mo with females having earlier onset • Greater $A\beta_{40}:A\beta_{42}$ in leptomeningeal vessels • Increased basement membrane thickness, loss of smooth muscle cells with weakened walls, and hemorrhages 	Xu et al. ⁷¹ Herzig et al. ⁷⁸
APPLd/2	n/a	15–25mo	<ul style="list-style-type: none"> • Decreased vascular $A\beta_{40}:A\beta_{42}$ • Significant CAA in leptomeningeal, cortical, thalamic, and hippocampal vessels • Thioflavin-s staining in severe vessels displayed concentric ring patterns • Congo red staining detected amyloid fibers in vessels • Vessels are dilated and pial arterioles exhibited aneurysms 	Van Dorpe et al. ⁸⁵
3xTg-AD	n/a n/a	10–11 mo	<ul style="list-style-type: none"> • Increased basal lamina thickness • Microvessels have less regular shape 	Bourasset et al. ⁸⁶
		3–18 mo	<ul style="list-style-type: none"> • Reduced cerebrovascular volume as early as 3–18 mo • Facilitated diffusion significantly reduced by 18 mo • Significantly lower GLUT-1 in capillaries 	Do et al. ²⁴

d: days; mo: months.

flow disturbances were observed in carotid arteries at 11 mo of age with significant flow voids in the major arteries of the Circle of Willis by 20 mo of age.^{45,47,48} Moreover, vascular casts showed areas devoid of vessels that were sites of thioflavin S-positive $A\beta$ plaques.

The size of the voids increased with age and were attributed to smaller voids progressing into a single larger cavity and thought to be sites of angiogenic processes^{48,49,53} (Figure 2). Additionally, the cavities appeared to preferentially cluster in the frontal and

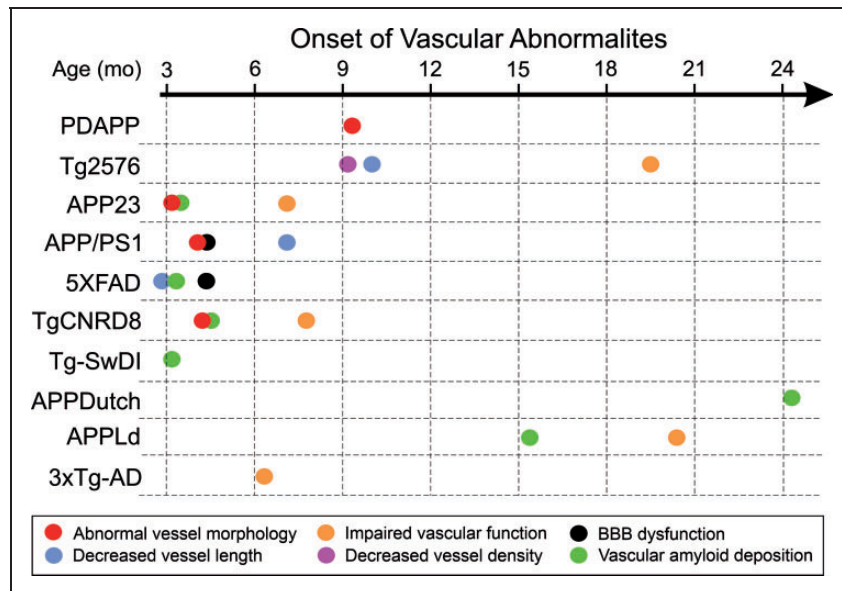


Figure 1. Summary timeline of vascular decrements in mouse models of AD. A schematic timeline detailing the age at which cerebrovascular deficits are first reported to appear. It is evident that cerebrovascular structure and function are impaired at early ages. Note that the occurrence of vascular amyloid also temporally coincides with altered vessel structure (green and red circles). Red: abnormal vessel morphology; blue: decrease in vessel length; purple: decrease vascular density; orange: impaired vascular function; black: BBB dysfunction; yellow: appearance of vascular amyloid.

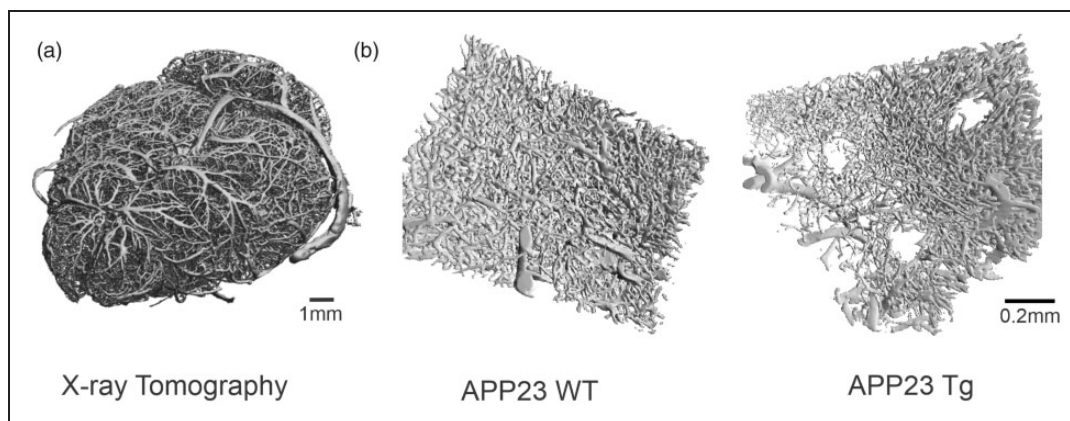


Figure 2. Vascular corrosion casts of APP23 mice. (a) High-resolution 3D reconstruction of a vascular cast acquired using X-ray synchrotron tomography ($17 \times 12 \times 7 \text{ mm}^3$ at $10 \mu\text{m}$ resolution) illustrating the dense vascular plexus in a control (wildtype, non-transgenic, age-matched) mouse. (b) Cortical vascular density is reduced and exhibits large voids in 12.7 mo old APP23 mice compared to age-matched WT controls. The vascular voids have been attributed to $\text{A}\beta$ deposition (see Meyer et al.⁴⁶). Images courtesy of T. Krucker, E.P. Meyer, M. Stampanoni, A. Obenaus. Images were acquired at the Swiss Light Source, Paul Scherrer Institute, Villigen, Switzerland.

temporal cortices,⁴⁶ mirroring a similar phenotype observed in human AD^{50,51} where early depositions of $\text{A}\beta$ were first detected in the frontal and temporal regions.^{54,55}

Abnormal $\text{A}\beta$ -positive structures, characterized as “pompons” (small fibrillary structures) and “cubes” (structures with flat, rough, and rounded surfaces), appeared in the casts of young (3–5 mo old) APP23

mice. Pompons and cubes were found colocalized to the same vessel and were often associated with capillary distortions. The authors suggested that pompons undergo morphological transformation to form cubes which later develop into large aggregates of vascular $\text{A}\beta$ deposits contributing to exacerbating vessel degeneration.⁴⁶ Similar morphological structures were also observed in capillaries of autopsied human AD brains

where small A β deposits are flat and ellipsoidal and found parallel to ECs while larger spherical A β deposits appeared to distort capillary lumens.³¹ Together, these findings strongly suggest that the presence of vascular A β prior to the manifestation of parenchymal A β plaques contribute to and possibly accelerate AD pathology.¹⁴

APP/PS1

APP/PS1 transgenic mice co-express FAD mutant human PS1 variant (A2463) and a chimeric mouse/human APP with Swedish FAD mutations (APP^{swe}). The co-expression in APP/PS1 transgenic mice results in accelerated production of A β plaques along with dystrophic neurites and reactive gliosis by 12 mo of age.⁵⁶ The vascular structure and architecture of APP/PS1 mice have been examined using vascular corrosion casting and SEM.^{57,58} Vascular casts from 4–5 and 9 mo old male APP/PS1 mice displayed microaneurysms along the length of the capillary or at bifurcation points⁵⁷ where extravasation of the casting solution was observed as “tags” on capillaries⁵⁸ indicative of BBB impairment. Similar to vascular casts from APP23 mice, casts from 4–5 mo old APP/PS1 mice also revealed discrete protrusions from capillary walls⁵⁷ further supporting the vascular hypothesis that abnormalities in the vasculature precedes the manifestation of AD. In stark contrast, casts from WT mice exhibited normal capillary networks with smooth luminal surfaces where visible elongated and rounded imprints of ECs on arteries and veins could be seen, respectively. Quantitatively, no significant differences in intracerebral arteriolar width nor capillary width or length was observed between genotypes.^{57,58}

In a recent study, high resolution mapping of the whole mouse brain cerebrovasculature was performed using the advanced Micro-Optical Sectioning Tomography (MOST) imaging in 24 mo old APP/PS1 male mice. Compared to WT mice, APP/PS1 mice displayed abnormal vessel morphology in the cortex and hippocampus where vessels appeared to be thinner, disorganized, and less uniform. In the hippocampus, vascular diameters and volumes were significantly lower compared to WT mice although no significant differences in vessel length were observed between genotypes. Specifically, greater vascular alterations were detected in subregions of the hippocampus including the dentate gyrus. For example, decreased vessel diameters and volumes were detected in the CA3 and the dentate gyrus while decreased vessel lengths were observed in the CA1-2 and dentate gyrus. Although APP/PS1 mice lack the hierarchical branching pattern observed in WT mice, they exhibited increased branching pattern with greater distal fine branches. APP/PS1

mice displayed significantly decreased branch angles which correlated with reduced cerebrovasculature spatial coverage. In addition to MOST imaging, virtual endoscopy was employed to visualize the vascular lumen. Compared with WT mice which displayed a smooth luminal surface and smooth circles at new branch points, APP/PS1 mice had a jagged appearance of their vascular lumen with an irregular lumen at new branch openings.⁵⁹ These abnormalities may significantly impair hippocampal CBF in this mouse model of AD.

Capillary parameters have also been quantified in the corpus callosum of 7 mo old male APP/PS1 mice. Beta-nicotinamide adenine di-nucleotide phosphate (NADPH)-diaphorase histochemistry was utilized for visualization of capillaries and computerized stereological approaches were employed to quantify various capillary parameters in the corpus callosum. Overall, compared with their WT counterparts, APP/PS1 mice had a 21% reduction in the total number of capillary segments (or branch points), suggesting that capillary length or density participates in the loss of capillary segments. Interestingly, no significant differences were found in the total capillary length or length density between APP/PS1 and WT mice. The volume of the corpus callosum was not statistically different between genotypes.⁶⁰

The reduced capillary segments may be due to increased vessel tortuosity (see Figure 3). Coincidentally, vessel tortuosity has been observed in the corpus callosum of human AD brains.^{50,51} Vessel tortuosity in the form of kinking or looping, is in part influenced by the anatomy of the vessel. For example, large vessels with no branch points may twist into one loop (where it appears as a C or S-shape) while smaller vessels with branches can exhibit more complex tortuous structures.⁶¹ Therefore, it is plausible that the reductions in capillary segments or branch points observed in APP/PS1 mice may lead to the microvessels having a single loop without gross changes in total capillary length or density.

Findings regarding BBB integrity in APP/PS1 mice have been conflicting. As described above, corrosion casts from 7 mo old male APP/PS1 mice exhibited extravasation of the casting materials from the vessels into the perivascular space, indicative of impaired BBB.⁵⁸ Consistent with this finding, enhanced Evans blue extravasation was observed in 12 mo old transgenic mice and electron microscopy revealed altered BBB integrity in the CA1 with loose tight junctions (TJs).⁶² Gadolinium-enhanced contrast magnetic resonance imaging (MRI) also revealed significant increases of hippocampal BBB permeability in 14 and 24 mo old male and female APP/PS1 mice.⁶³ In contrast, studies using *in situ* brain perfusion did not detect any

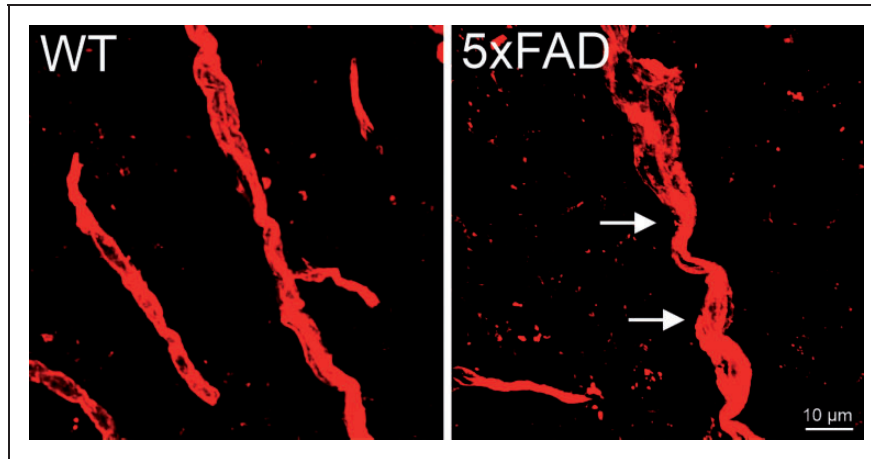


Figure 3. Cortical vessels in 5xFAD mice appear more tortuous. Increased vessel tortuosity was observed in the cortex of 8 mo old 5xFAD female mice. In WT mice, vessels appear more linearly oriented perpendicular to the cortex while in the same cortical region vessels from 5xFAD mice appear more tortuous (arrows). Vessels were stained with tomato lectin. 5xFAD mice were provided by the MODEL-AD consortium at University of California Irvine.

difference in the integrity and function of the BBB in 8 mo old APP/PS1 mice compared to controls. The vascular volume in the hippocampus and the total hemisphere, as measured with [14 C]-sucrose, was unchanged between WT and transgenic mice. Moreover, passive and facilitated diffusion across the BBB measured by [3 H]-diazepam and [3 H]-D-glucose, respectively, were similar in controls and APP/PS1 mice²⁴ suggesting an intact BBB structure and function. Similarly, lack of BBB dysfunction was not observed in 5–12 mo old APP/PS1 male mice after bolus injection of human A β_{40} .⁶⁴ *In vivo* two-photon imaging also did not reveal any differences in blood vessel volume in 15 mo old APP/PS1 and control mice. However, a marked increase in blood vessel volume was observed when APP/PS1 mice were crossed with the tauopathy mouse line, Tg4510 (APP/PS1-Tg4510), suggesting that amyloid plaques alone do not contribute to vascular changes in AD.⁶⁵ Thus, it is not clear if the vascular alterations in APP/PS1 mice definitively lead to disruptions to the BBB. Alternate explanations include differences in the mouse strain background, among others.

5xFAD

The 5xFAD mice were generated to facilitate rapid development of A β plaques using APP/PS1 double transgenic mice that co-express five FAD mutations (APP K670N/M671L (Swedish), I716V (Florida), V717I (London), and two PSEN1 mutations (PS1 M146L and L286V) under control of mouse *Thy1* minigenes. These mice express intraneuronal A β_{42} as early as 1.5 mo of age with progressive A β depositions and gliosis as early as 2 mo of age. Female 5xFAD mice

also express more APP than their male counterparts due to the estrogen response element in the *Thy1* promoter,⁶⁶ which could contribute to the more severe phenotype in female mice. Moreover, loss of synaptic markers, accompanied by memory impairments are also observed in these mice.⁶⁷

Alterations in vessel morphology have been observed in 5xFAD mice where changes in microvasculature appeared first in the fronto-parietal cortices and later in the hippocampus⁶⁸ paralleling A β accumulation that appears first in the cortices and later in the dentate gyrus.⁶⁷ Compared to controls, 8–9 mo old female 5xFAD mice vessels had a damaged and deteriorated morphology^{69,70} with “scratches” along the vessels.⁶⁹ In our own preliminary findings, we observed also tortuous cortical vessels in 8 mo old 5xFAD female mice (Figure 3).

Not surprisingly, abnormal morphology of the cerebrovasculature can impair and damage vessels. FITC-albumin labeled microvessels revealed capillary leakage appearing at 4 mo of age which became more prominent by 9 and 12 mo of age in 5xFAD female mice compared to controls.⁶⁸ Similar findings were also observed in 8 mo old 5xFAD mice, where reconstructed 3D super resolution structured-illumination microscopy (SIM) images showed disconnected short length cortical capillaries where TJs also exhibited significantly shorter lengths as compared with WT mice.⁷⁰ Prominent loss of TJ protein zona occludens-1 (ZO-1) have been reported in these transgenic mice.⁶⁹ Furthermore, cultured ECs incubated with A β_{42} displayed significant reductions in ZO-1 and claudin-5⁷⁰ suggesting that amyloid deposition can disrupt expression of TJs proteins, leading to increased BBB permeability.

Changes in the cerebrovascular density have also been quantified in 5xFAD mice. Reductions in microvascular length have been reported as early as 2 and 4 mo of age⁶⁸ which coincides with the timing of intra-neuronal and parenchymal A β accumulation.⁶⁷ Significant reductions in brain vessels, as measured by levels of GLUT-1, were also observed in 9 mo old female 5xFAD mice.⁶⁹ Similar pathological alterations in the cerebrovasculature have also been investigated in postmortem human AD brains.^{50,51} Staining against heparin sulfate proteoglycan, a glycoprotein found in the vascular basement membrane and in amyloid deposits, revealed decreased microvessel density, reductions in cortical vessel length, and overall loss of angioarchitecture. Decreases in microvessel density could be due to the observed string (thinned) vessels and fragmented microvessels with loss of intact branches.^{50,51}

While structural changes of the cerebrovasculature have been documented, the timing and accumulation of CAA is variable in 5xFAD mice. *In vivo* two-photon imaging revealed Methoxy-XO4 positive amyloid deposits in the leptomenigeal and penetrating cortical vessels in 5xFAD female mice as early as 3 mo of age which progressed with aging, although CAA observations were limited to microvessels.⁶⁸ Detection of thioflavin-S positive A β in blood vessels has also been difficult. For instance, 3 and 6 mo old 5xFAD mice lack thioflavin-S positive vascular A β .⁷¹ In our studies, we did not detect any thioflavin-S positive vascular amyloid in 4 and 8 mo old 5xFAD mice and minimal thioflavin-S positive vascular amyloid in larger

cortical vessels of 12 mo old 5xFAD mice (Figure 4). The limited thioflavin-S positive vascular amyloid deposits could be attributed to the molecular composition of A β plaques present in these mice. For example, thioflavin-S staining is positive in amyloid containing fibrillar content with β -pleated sheet conformation⁷² and findings have demonstrated greater dense core A β plaques and reduced fibrillary amyloid in 5xFAD mice.⁷³

TgCRND8

The early onset TgCRND8 mouse encodes a double mutant form of APP695 under the PrP promoter. These mice develop A β plaques at 3 mo of age with plaque load increasing with age and an excess of A β_{40} and A β_{42} by 6 mo of age.⁷⁴ Specifically, TgCRND8 mice exhibit significantly more A β_{40} load in vessel-depleted cortices than in isolated blood vessels compared to A β_{42} . CAA development was apparent in 4 mo old mice which increased with age and exhibited thioflavin-S positive cortical blood vessels. Furthermore, *in vivo* two-photon imaging revealed striking differences in the arterioles between transgenic and non-transgenic mice with arteriole abnormalities increasing with age in transgenic mice. Specifically, TgCRND8 mice exhibited greater arteriolar tortuosity and curvature with smaller arteriolar radii.³⁰ Increased tortuosity of small arterioles, primarily in the white matter, has also been reported in human AD.^{50,51} To confirm whether vascular A β was correlated with increased tortuosity, TgCRND8 mice were administered prophylactic treatment of scyllo-inositol to

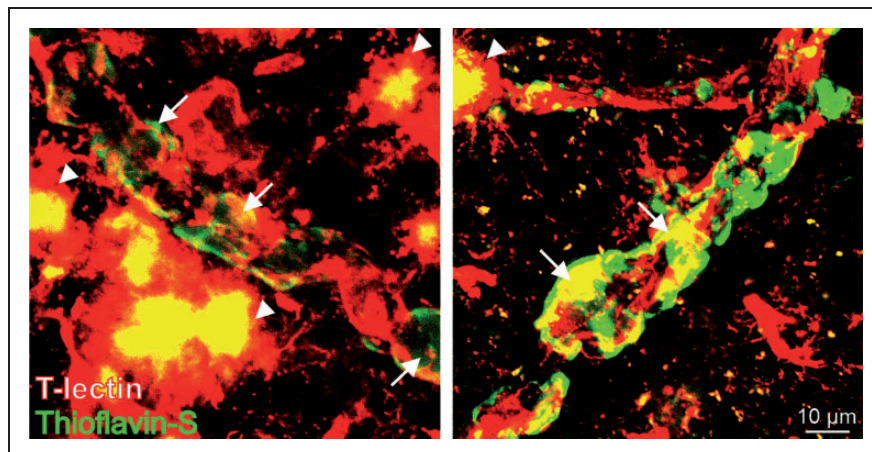


Figure 4. Vascular amyloid deposition in 5xFAD mice. Two examples of vascular amyloid deposition from 12 mo old 5xFAD mice. Left Panel: A β plaques (thioflavin-S, arrows) are observed wrapping around cortical vessels stained with tomato lectin. Large apparent aggregates of degenerating or dissolved amyloid encased vessels are also observed (arrow heads). Right Panel: Another example of dramatic aggregates of A β (thioflavin-S; green; arrows) surrounding a T-lectin-stained vessel. In this example the vessel appears more intact compared to the vessel in left panel. Interestingly, A β deposition is not uniform in all vessels with some vessels preferentially affected. (tomato lectin, blood vessels; red), thioflavin-S (A β ; green). 5xFAD mice were provided by the MODEL-AD consortium at University of California, Irvine.

target A β oligomers *in vivo*, which significantly reduced tortuosity, confirming that A β plaques and oligomers cause vessel tortuosity and prevention of these plaques and oligomers can restore normal vessel morphology.³⁰

To determine the role of A β on vascular function, microvascular network efficiency was assessed. In late-stage CAA, the microvascular transit time was significantly longer in TgCRND8 mice compared to non-transgenic mice and scyllo-inositol treated TgCRND8 mice. Compared with non-transgenic mice and scyllo-treated mice, the transit time dispersion was higher in TgCRND8 mice in both air-breathing and hypercapnia indicating that A β impaired the functional efficiency of the vascular network and that prevention of A β oligomerization and deposition can restore vascular function. During the hypercapnic challenge, control mice exhibited shortened transit times as expected, whereas elongated transit times were observed in the transgenic mice.³⁰ The increased transit time reported in the TgCRND8 mice may be due to the preserved venous dilation³⁰ as amyloid depositions are more commonly found on arterioles rather than venules.⁷⁵

In addition to arteriole pathology, structural and functional venule degeneration has also been observed, where 7 mo old TgCRND8 mice compared to 5 mo old TgCRND8 mice, exhibited a significant decrease in mural cell coverage in penetrating venules.⁷⁶ Intracerebroventricular delivery of SU6668, an antagonist for PDGFR β activity in TgCRND8 exacerbated arteriolar amyloid accumulation as well as significant loss of mural cell coverage on penetrating vessels. Surprisingly, *in vivo* two-photon imaging revealed increased coiling and looping in veins but not arteries in SU6668 treated TgCND8 mice, suggesting that loss of mural cell coverage leads to structural changes only in venules. Significant increases in PDGFR β , S100 β , and AQP4 expression levels were observed in TgCND8 mice treated with SU6668 suggesting a compensatory mechanism relating to BBB integrity. Consistent with previous findings,³⁰ attenuated flow responses to a hypercapnic challenge were observed in TgCND8 mice while SU6668 treated mice had increased venular flow indicating partial restoration of venular activity⁷⁶ which may be due to preserved venous dilation, as previously suggested.³⁰

Tg-SwDI

The Tg-SwDI strain is a triple transgenic expressing the human neuronal amyloid precursor protein containing Swedish K670N/M671L and vasculotropic Dutch (E693Q) and Iowa (D694N) mutations (numbering based on the APP₇₇₀ isoform) under the mouse Thy1.2 promoter.⁷⁷ These mice are unique in that they develop early-onset A β in the cerebral

microvessels which increases with age.^{71,77} At 3 mo of age, significant increases in both A β ₄₀ and A β ₄₂ are observed in isolated microvessels of the forebrain which increases dramatically by 12 mo of age. At 6 mo of age, accumulation of A β is observed in and around microvessels, particularly in the thalamus and subiculum. The arterioles in these brain regions and in the hippocampal fissure exhibit robust vascular and perivascular A β deposits. Additionally, microhemorrhages were detected on microvessels adjacent to A β deposits.⁷⁷

APPDutch

The recently generated APPDutch strain is the only mouse model of AD that develops significant CAA with little or no parenchymal amyloid plaques. APPDutch mice were developed by overexpressing the human APP751 harboring the E693Q mutation under the control of neuron-specific murine Thy-1 promoter. One disadvantage of this mouse model is the late onset of cerebrovascular amyloid which appears at ~22–25 mo old with females displaying earlier onset compared to males. APPDutch mice develop CAA first in the leptomeningeal vessels with a greater ratio of A β ₄₀:A β ₄₂. Increased basement membrane thickness, loss of VSMCs with weakened vessel walls, and hemorrhages were observed in these mice. This demonstrates that neuron-derived A β can be transported to the cerebrovasculature where it leads to significant deposition of vascular amyloid and degeneration of VSMCs.⁷⁸ Studies crossing APPDutch mice with other transgenic mouse models have been performed. For example, female APPDutch mice crossed with transgenic mice overexpressing BACE (APPDutch/BACE1) revealed similar levels of amyloid-laden cortical vessels as the APPDutch mice at 22 mo old, although significant thalamic vascular amyloid deposition was observed in APP/BACE1 compared with APPDutch mice.⁷⁹ Further, APPDutch mice crossed with APP23 (APPDutch/APP23) mice led to significant vascular amyloid load and hemorrhage compared to APP23 mice at 24 mo of age.⁸⁰ Both APPDutch/BACE1 and APPDutch/APP23 have greater levels of A β ₄₀ compared with A β ₄₂.^{79,80} These findings indicate that A β ₄₀ Dutch mutation drastically reduces parenchymal amyloid plaques but is sufficient for CAA induction.

APP/Ld/2

The APP/Ld/2 mouse model of AD overexpresses the common human APP695 V717I London mutation under the murine Thy-1 promoter.⁸¹ Studies showed that V717I missense mutation modifies γ -secretase

cleavage resulting in an increased ratio of $A\beta_{42}$: $A\beta_{40}$.^{82–84} Like APPDutch mice, APP/Ld/2 mice exhibit significant vascular amyloid deposition. However, unlike the APPDutch mice, APP/Ld/2 mice also contain neuritic and diffuse plaques, as is seen in human patients. Biochemical analysis in 15–24 mo old APP/Ld/2 mice found a decreased ratio of $A\beta_{42}$: $A\beta_{40}$ in the vasculature. Thioflavin-S staining revealed $A\beta$ in the leptomeningeal, cortical, thalamic, and hippocampal vessels which increased with age. Vessels with increased thioflavin-S staining exhibited a pattern of concentric rings,⁸⁵ similar to the TgCNRD8 mouse model.³⁰ On the other hand, Congo red staining detected the presence of amyloid fibers in vessels with vascular amyloid appearing first in the pial arterioles while veins and capillaries had minor accumulations of $A\beta$. Notably, amyloid was absent in the main branches of the middle cerebral, anterior cerebral and posterior communicating arteries, although smaller branches exhibited high accumulation of $A\beta$. Transmission electron microscopy revealed dilated vessels and aneurysms of pial arterioles, but hemorrhages were not detected. In response to a hypercapnic challenge, 20–24 mo old APP/Ld/2 mice exhibited a similar increase in CBF compared to WT mice suggesting that the vasodilatory properties of the cerebrovasculature was maintained despite increased vascular amyloid load in these mice.⁸⁵

Transgenic mouse line with $A\beta$ plaques and neurofibrillary tangles

3xTg-AD

The triple-transgenic model (3xTg-AD) was the first transgenic mouse line to develop both $A\beta$ plaques and NFTs. These mice were generated using pronuclear microinjection where two transgenes were injected into single-cell zygotes from homozygous *Psen1*_{M146V} mice. 3xTg-AD mice develop extracellular $A\beta$ plaques prior to formation of NFTs and exhibit age-dependent impairments in synaptic plasticity before the manifestation of $A\beta$ depositions and tangles.³

Functionally, 3xTg-AD mice exhibit reductions cerebrovascular volume, particularly in the hippocampus, where decreases begin as early as 6 mo of age²⁴ and have been observed up to 11 mo of age.⁸⁶ The uptake of [³H]-diazepam was found to be similar to control mice suggesting normative passive diffusion.^{24,86} In contrast, facilitated diffusion, as measured by *in situ* perfusion of [³H]-D-glucose, was significantly reduced at 18 mo of age.²⁴ The decrease in brain uptake of D-glucose may be attributed to the loss of GLUT-1, as 3xTg-AD mice exhibit significantly lower brain GLUT-1 in capillaries.²⁴ Thus, alterations in cerebrovascular volume and facilitated diffusion across the BBB may contribute to

both amyloid and tau pathology which worsen with aging.

Mechanisms of vascular amyloid clearance

The presence of parenchymal and vascular $A\beta$ clearly leads to marked changes in both the structure and function of the cerebrovasculature. Mounting evidence suggests that vascular $A\beta$ may play an integral role in the development of AD and that the lack of $A\beta$ clearance from the cerebrovasculature can exacerbate AD pathology.⁸⁷ $A\beta$ homeostasis in the brain is regulated by a multitude of pathways which can influence disease progression (e.g., early or late onset).⁸⁸ Indeed, failure of appropriate $A\beta$ elimination from the cerebrovasculature is considered a primary factor in the etiology of AD and CAA (Figure 5).

Studies have shown that transvascular clearance of $A\beta$ across the BBB is the predominant mechanism of $A\beta$ elimination.⁸⁸ In human AD brains, BBB disruption is correlated with AD pathology and cognitive impairments.⁸⁹ At the level of the BBB, the receptor for advanced glycation end products (RAGE) is the key transporter of $A\beta$ across the BBB into the brain while the low-density lipoprotein receptor-related protein-1 (LRP-1) aids in clearance of $A\beta$ from brain to blood.⁹⁰ Besides their interaction with $A\beta$, RAGE and LRP-1 are also expressed by various cell types.⁹¹ While a vast body of evidence has revealed altered cellular expression of RAGE and LRP-1 in association with AD, there is little evidence on how these proteins are altered within the vasculature itself. In humans, significant increases in vascular RAGE expression have been documented in individuals with advanced AD. Compared with autopsy controls and early AD, brains from severe AD individuals displayed robust microvascular RAGE immunoreactivity in the hippocampus.^{90,92,93} It is not surprising then, that the upregulation of RAGE can alter CBF. Indeed, infusion of $A\beta$ in mice, not only confirmed RAGE-mediated transport of $A\beta$ across the BBB, but also provided evidence of decreased CBF, which may be caused, in part, by an increase in endothelin-1 (ET-1), a known potent vasoconstrictor.⁹⁴ Increased ET-1 in reactive astrocytes have been previously reported in AD cases, but the significance of these findings remains to be clarified.^{95,96} Together, these findings strongly suggest that increased RAGE may coincide with increased brain amyloid burden and contribute to vascular amyloidosis.

In contrast to increased RAGE, downregulation of vascular LRP-1 has been observed and is thought to contribute to impaired $A\beta$ clearance. In the hippocampus of AD patients, weak LRP-1 immunoreactivity was detected in microvessels compared to autopsy controls

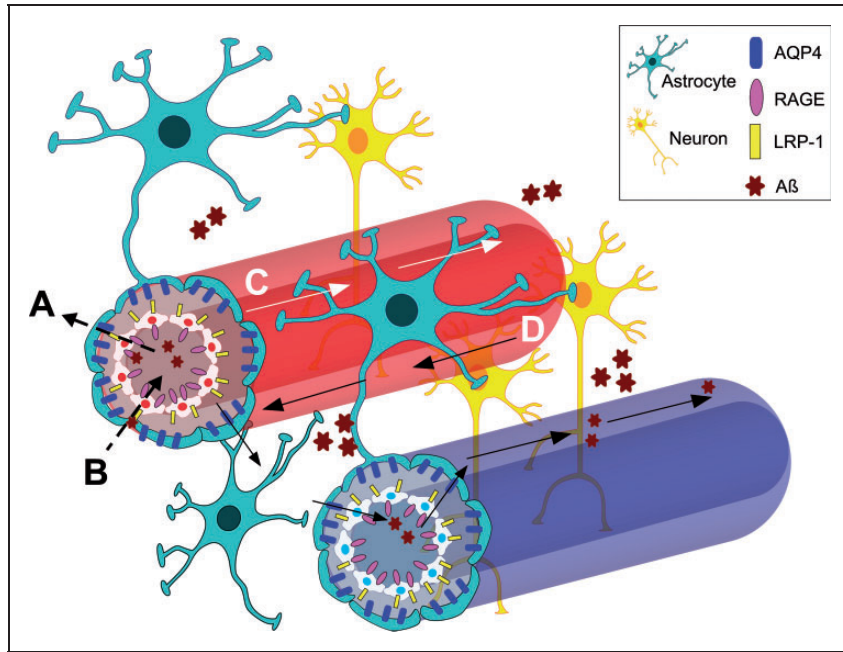


Figure 5. Proposed mechanisms of vascular amyloid clearance. (A) Vascular RAGE, expressed by endothelial cells, is the key transporter of A β across the BBB into the brain. Upregulation of RAGE is observed in severe AD brains. (B) Vascular LRP-1, expressed by endothelial cells, aids in clearance of A β from brain to blood. Downregulation of LRP-1 is observed in brains of AD patients. (C) Soluble A β is drained via the perivascular route along the arterial basement membrane and towards the leptomeningeal arteries. (D) A β is cleared through the 'glymphatic system' in which soluble A β is cleared via bulk flow facilitated by AQP4. RAGE = receptor for advanced glycation end products, LRP-1 = lipoprotein receptor-related protein-1, AQP4 = aquaporin-4.

which had strong LRP-1 staining.⁹⁰ Evidence of impaired A β clearance due to decreased LRP-1 in human and mouse VSMCs has been reported. Knockdown of LRP-1 using siRNA in human brain vascular smooth muscle cells significantly increased endogenous A β_{40} and A β_{42} , while conditional deletion of *Lrp1* in VSMCs of APP/PS1 mice exacerbated A β deposition in the cortex and leptomeningeal arteries.⁹⁷ Additionally, antisense targeted against LRP-1 mRNA in mice resulted in reduced A β_{42} clearance at the BBB with increased parenchymal A β_{42} and learning and memory deficits in mice.⁹⁸ These and other studies strongly support the neurovascular hypothesis of AD.⁹⁹

Another accepted mechanism of amyloid clearance is via perivascular drainage of solutes and interstitial fluid (ISF). As soluble A β enters the basement membrane of capillaries it is subsequently drained along the arterial basement membrane toward the leptomeningeal arteries. The force for perivascular drainage is thought to arise from arterial pulsations.¹⁰⁰ Confirmation of this pathway has been demonstrated using fluorescent tracers injected into the corpus striatum of 6–8 wk old adult MF1 mice where tracer molecules initially diffused throughout the brain parenchyma and drained along the basement membrane of capillaries and arteries. Little or no tracer

molecules were detected in veins. While no evidence of the tracer was detected in the leptomeningeal arteries it was present in perivascular macrophages surrounding leptomeningeal arterial walls suggesting that the tracer had moved through the leptomeningeal arteries and out of the brain.^{101,102} These and other findings suggest that the meningeal lymphatic vessels are key players in the removal of macromolecules from the CNS and into the cervical lymph nodes. After ablation of meningeal lymphatic vessels in normal aging wild-type (WT) mice, injected fluorescent tracer molecules did not reach the deep cervical lymph nodes and diffusion of the fluorescent tracer molecules into the brain along the blood vessels was reduced. Interestingly, reductions in meningeal lymphatic vessel diameter and coverage were observed in 20–24 mo WT mice. Destruction of meningeal lymphatic vessels in 5xFAD mice led to accelerated A β deposition in the meninges and parenchyma as well as cognitive deficits, similar to those in human AD brains.¹⁰³ Thus, these studies signify a key role of the leptomeningeal arteries in the clearance of A β via the perivascular drainage pathway.

Reductions in perivascular drainage were also associated with increased thickness of the vascular basement membranes which occurred in an age-dependent manner.¹⁰² Significant increases in capillary basement membrane thickness in the cortex, hippocampus, and

thalamus were observed in 23 mo old WT mice compared to 2 and 7 mo old mice. Injection of soluble human A β ₄₀ revealed reductions in perivascular drainage that was more prominent in the hippocampus compared to the thalamus, again consistent with the concept that vascular amyloid impairs perivascular drainage.¹⁰⁴ Thus, the efficiency of perivascular drainage appears to differ between brain regions.

Subsequent studies further investigated perivascular drainage in the hippocampus.¹⁰² Intracerebral injections of fluorescent dextran in WT mice revealed significant impairments in perivascular drainage in hippocampal capillaries and arteries of 22 mo old mice compared to 3 and 7 mo old mice. This deficit was correlated with age-related changes in capillary density and increased vascular basement membrane thickness. As noted above, age related drainage appeared to be within the arterial system but intracerebral injections of fluorescent dextran in Tg2576 mice revealed a significant increase in dextran-positive hippocampal veins of 22 mo old mice compared to 3 and 7 mo old mice while no significant differences in dextran labeling of hippocampal capillaries and arteries between ages were found.¹⁰² The absence of dextran labeling in the capillaries and arteries were attributed to reductions in capillary density which has been observed in other mouse models of AD.^{38,105,106} However, the increased dextran labeling in veins suggests that vascular amyloid deposition altered the normal route of perivascular drainage. In support of this, no significant differences in large diameter vessel density was observed between ages in Tg2576 mice or in WT mice. If perivascular drainage is indeed driven by arterial pulsations, then it is likely that this driving force may be lost due to impairments in CBF dynamics. As described above, Tg2576 mice have reduced CBF and deficits in vasodilatory and vasoconstrictive properties.⁴⁰ These findings would imply that perivascular drainage is not only impaired with aging but that increased severity of CAA further contributes to disruptions of A β perivascular drainage.

Recently, a new mechanism of A β elimination has been proposed which has garnered widespread interest. This pathway of A β removal is thought to be along the paravascular routes. Because the brain parenchyma lacks lymphatic vessels, a “glymphatic system” for waste and solute removal has been suggested.¹⁰⁷ The glymphatic pathway posits that interstitial solute clearance, such as A β , is driven by convective bulk flow. Using various small fluorescent tracers, it was found that influx of the cerebrospinal fluid (CSF) is along para-arterial routes and efflux of ISF is along paravenous routes facilitated by the astrocytic water channel aquaporin-4 (AQP4). Injection of radiolabeled and fluorescently tagged A β was shown to move along

the vasculature and accumulate in the capillaries and large draining veins. Furthermore, radiolabeled A β clearance was reduced by ~55% in the absence of AQP4 suggesting that AQP4 plays a role in soluble A β clearance via bulk flow. However, this mechanism of solute clearance has been highly debated.^{108,109} In one study, the distance by which the intensity of fluorescent-tagged A β was decreased from the injection site was similar in both WT and mice lacking AQP4, indicating that AQP4 does not aid in bulk flow A β clearance.¹¹⁰ These and other controversial findings regarding A β clearance through the glymphatic pathway warrant additional investigations.

Impact of a dysfunctional neurovascular unit on AD cerebrovasculature

It is evident that failure of amyloid clearance can manifest specific cerebrovascular phenotypes. However, it remains unclear how vascular amyloid deposition molds surrounding cells to alter vessel morphology and function. The cerebrovascular network is a complex and dynamic system composed of various cell types including neurons, astrocytes, pericytes, ECs, and VSMCs.¹¹¹ Coined as the neurovascular unit (NVU, or expanded NVU¹¹¹), these cells work synergistically to maintain central nervous system (CNS) homeostasis.¹¹¹ Along with tight and adherens junctions, the ECs of the NVU comprise the BBB to facilitate transport of nutrients and provide a barrier against harmful molecules.¹¹² Emerging evidence suggests that damage to constituents of the NVU likely plays a significant role in the pathophysiology of AD, further supporting the vascular AD hypothesis. While little is known on how cells of the NVU directly remodel the cerebrovasculature in AD, it is well established that a dysfunctional NVU can generate a cascade of events, ultimately leading to reductions in CBF, increased BBB leakage, and associated complications that have been reported in AD²² (Figure 6).

Marked disturbances in vessel architecture and function can be also be attributed to changes in VSMCs and ECs. In postmortem AD brains, morphological changes of the cerebral vessels were attributed to irregularly shaped and swollen ECs and deteriorating VSMCs.^{113,114} The ability of these cells to synthesize and release soluble A β may also be one mechanism on how neurodegenerative processes are further exacerbated in AD. In an early study, cultured human VSMCs incubated with A β ₁₋₄₂ not only caused degeneration of VSMCs but also led to induction of cellular APP which can lead to an increase in soluble A β levels.¹¹⁵ On the other hand, ECs are able to synthesize the neurotoxin thrombin¹¹⁶ which can induce APP

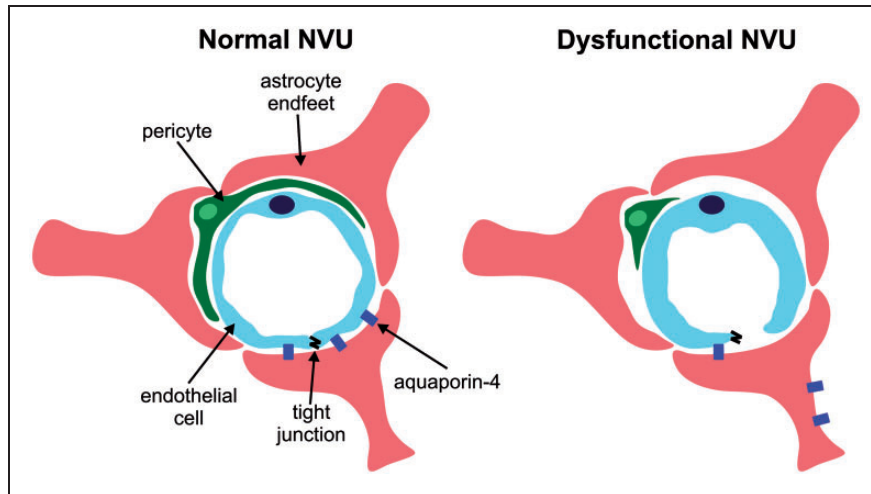


Figure 6. Development of a dysfunctional neurovascular unit (NVU) in AD. In the normal NVU (left), pericytes, astrocytes, and endothelial cells, work synergistically to maintain homeostasis and provide a barrier against harmful molecules. In the AD brain, a dysfunctional NVU may develop from swollen endothelial cells, loss of pericytes, impaired BBB, and mis-localization of aquaporin-4. These deficits can lead to consequences such as decreased BBB integrity, impaired A β clearance, altered vessel morphology, and compromised cerebrovascular functions. BBB = blood-brain barrier.

through PKC-dependent mechanism.¹¹⁷ Thus, a positive feedback loop may exist in which initial amyloid deposition causes VSMC and EC dysregulation leading to synthesis of additional A β ultimately resulting in the progression of AD.

Although reactive astrocytes are a common pathological feature present in both human and animal models of AD,¹¹⁸ their contribution to cerebrovascular dysfunction and ultimately disease progression remains largely unknown. One potential target is the astrocytic water channel aquaporin 4 (AQP4). In support of this, deletion of *Aqp4* in APP/PS1 and 5xFAD mouse models of AD showed significant increases in accumulation of parenchymal and vascular A β load,^{73,119} increased neuronal and astrocyte toxicity,^{73,119,120} and reduced A β uptake.¹²⁰ Perivascular AQP4 redistribution has also been observed in both rodent and human AD.^{36,73,119,121–123} Specifically, severe vascular A β deposition resulted in redistribution of AQP4 from the endfeet towards the neuropil away from the vasculature.^{36,121,122} These findings suggest that AQP4 dysfunction is complicit in NVU impairments and accelerates AD progression, ostensibly through a compromised BBB. In fact, several studies have demonstrated a role of AQP4 in BBB maintenance¹²⁴ and that redistribution or downregulation of AQP4 results in increased BBB leakage.¹²⁵

Pericytes are thought to play a role in vascular stability¹²⁶ and pericyte degeneration modulates cerebrovascular structure and function in AD.¹²⁷ A striking “string vessel” morphology (thin microvessels that lack ECs) are thought to be a consequence of pericyte

loss¹²⁸ and has also been observed in human AD brains.¹²⁹ Loss of pericyte coverage on blood vessels were observed in 8 mo old 5xFAD mice (Figure 5). In mice that overexpress *APP^{sw/0}* leading to reduced pericytes (*APP^{sw/0} Pdgfr β ^{+/-}*).¹³⁰ *APP^{sw/0} Pdgfr β ^{+/-}* mice exhibited significant accumulation of A β ₄₀ and A β ₄₂ in the cortex and hippocampus resulting in loss of A β clearance via the BBB¹³⁰. Not surprising was the significant increase of CAA in these mice as well as accelerated AD pathology which appears to contribute to increased BBB breakdown and subsequent cerebrovascular functional deficits.¹³⁰ A compromised BBB can have severe outcomes including accumulation of perivascular IgG, hemosiderin, thrombin, and plasmin,¹³¹ toxic macromolecules, all of which are known to play key roles in memory impairment¹³² and vascular damage¹³³ that are associated with AD.^{132,134}

Cerebrovascular targets for AD treatment

Despite exhaustive research efforts, a successful treatment for AD remains elusive. This may be attributed to the fact that current drugs are targeted towards directly reducing amyloid and tau aggregation, centered around the amyloid hypothesis.¹³⁵ It is now evident that accumulation of amyloid plaques and NFTs, even at early stages, can lead to vascular structural abnormalities which can ultimately lead to functional deficits. Thus, an alternative treatment option would be to reestablish normal vascular architecture in hopes of mitigating AD pathology. One study to date has demonstrated that cerebral microvascular architecture can

be restored pharmacologically with Liraglutide,⁵⁸ a glucagon-like peptide-1 (GLP-1) agonist used for the treatment of type 2 diabetes.¹³⁶ GLP-1 has been shown to cross the BBB¹³⁷ and be neuroprotective.¹³⁸ Daily injections of Liraglutide for 8 wk improved vessel architecture in 9 mo old APP/PS1 mice, including BBB integrity and vessel diameters comparable to controls.⁵⁸ In vehicle treated APP/PS1 mice, vessels were abnormal with evidence of increased vessel permeability. Thus, while treatment with Liraglutide shows promise in restoring cerebrovascular architecture, further studies are required to determine if the functional aspects of these vessels are also improved.

Another target for cerebrovascular directed therapy is the transferrin receptor (TfR) which is highly expressed by brain capillary endothelial cells (BCECs).¹³⁹ Transferrins are iron-binding blood plasma glycoproteins involved in iron homeostasis.¹⁴⁰ Abnormal accumulation of iron has been reported in the brains of AD patients¹⁴¹ and was correlated with the presence of A β plaques and hyperphosphorylated tau.¹⁴¹ Several studies have demonstrated the potential of TfR as a vector for drug delivery in the brain. For example, systemic or intravenous injections of monoclonal antibodies against TfR alone or conjugated to nanoparticles were shown to internalize into BCECs^{142–145} thereby allowing for controlled drug delivery. One exemplar study employed poly(lactico-glycolic acid) (PLGA) nanoparticles targeted with anti-TfR antibodies for improved drug transport across the BBB.¹⁴⁵ Here, nanoparticles with anti-TfR antibodies were used to deliver encapsulated iA β ₅, a peptide that binds to A β to inhibit the formation of the oligomer β -sheet¹⁴⁶ in cultured porcine BCECs.¹⁴⁵ Compared to nanoparticles without functionalized anti-TfR, the cellular uptake of nanoparticles targeted with anti-TfR was enhanced significantly. Critically, TfR levels were found to be similar between AD patients relative to controls^{142,147} and no significant differences in TfR levels were detected in 12–18 mo old 3xTg-AD¹⁴² or in 5 mo old PS2APP mice.¹⁴⁷ Thus, the ability of TfRs to act as nanocarriers for drug transport as well as the preservation of TfR in both human AD and mouse models of AD would suggest that TfR may be a good target candidate for drug delivery approaches.

Although autopsy remains the clinical gold standard for identifying the underlying pathology of AD, the aforementioned studies significantly highlight the cerebrovasculature as potential target for drug treatments. Thus, diagnostic procedures that can detect vascular changes associated with AD can be highly beneficial in testing new evolving therapeutics.

Conclusions

Accumulating evidence validates that cerebrovascular deficits are associated with AD, supporting the vascular hypothesis. Additionally, evidence has demonstrated that cerebrovascular dysfunction precedes AD pathophysiology. Hence, the two-hit hypothesis of AD could be modified wherein vascular factors combined with genetics result in vascular damage (hit 1) which is then followed by A β decrements in clearance along with APP processing (hit 2).²⁵ Despite considerable research, the underpinnings of AD remain to be elucidated; nonetheless, the studies reviewed herein seem to indicate that the cerebrovasculature is a highly vulnerable target that is implicated in AD disease progression.

In critically reviewing these studies, it is now clear that the cerebrovasculature undergoes drastic architectural changes well in advance to the accumulation of A β plaques. Moreover, severe A β plaque deposition and hyperphosphorylated tau lead to serious vascular disruptions. Profound structural changes such as looping, twisting, and kinking of blood vessels are expected to dramatically influence the regulation of CBF. In this cascade of pathology, vascular amyloid deposition can further exacerbate AD pathology by increasing BBB leakage which further alters CBF regulation. Clinical and experimental (preclinical) AD studies have reported impaired cerebrovascular function, which further confirms the importance of vascular health in abating the progression and pathophysiological mechanisms underlying AD. However, cerebrovascular decrements have focused primarily on changes in arteries and capillaries and attention to venule pathology has been largely overlooked. Indeed, venular amyloid have significant consequences on AD pathology¹⁴⁸ and evaluation of both arteriole and venule aberrations should be seriously considered in future studies.

The effects of vascular amyloid or CAA are of immense clinical importance. Expansion of research efforts investigating the cerebral vasculature are direly needed to gain a better understanding of the vascular mechanisms underlying the pathophysiology of AD. Increasing our understanding of the vascular progression leading to AD will enable future novel interventional treatment strategies. While we have not discussed inflammation within the context of this review, it is clearly important to consider how the inflammatory response, either within the parenchyma or within vessels, could impact the pathological progression. It is conceivable that treatments to blunt or reverse AD will require a combination of treatments, targeting diverse physiological responses. Thus, as a first step, rigorous characterization of the

cerebrovasculature, including the NVU, is crucial to clearly define its impact on AD symptomology and pathology.

While significant AD research has been undertaken, challenges remain due to variability in study methods (i.e., animal models, age, methodology, parameters, etc.). These differences between studies make comparisons almost impossible and future research should consider employing similar criteria and utilize common data elements (CDEs) to ensure standardization and harmonization across investigators. The use of “collaborative crosses”¹⁴⁹ in preclinical disease models may also provide crucial information on how natural genetic variation influences vascular decrements in AD. Overall, generation of reliable and complete data will further significant advancement in the field of AD research.

Funding

The author(s) disclosed receipt of the following financial support for the research, authorship, and/or publication of this article: MODEL-AD was established with funding from The National Institute on Aging (U54 AG054345-01, U54 AG054349-01).

Declaration of conflicting interests

The author(s) declared no potential conflicts of interest with respect to the research, authorship, and/or publication of this article.

ORCID iD

André Obenaus  <https://orcid.org/0000-0003-0081-6950>

Acknowledgements

The authors wish to thank members of the UCI MODEL-AD consortium for providing stimulating discussions about Alzheimer’s Disease and how the cerebrovasculature impacts onset and progression of the disease (www.model-ad.org). The authors also wish to acknowledge the UCI MODEL-AD for providing AD mouse models for investigation of the vessel architecture. The authors thank Drs. Thomas Krucker (Novartis Institutes for BioMedical Research, Inc.), David Cribbs (University of California Irvine) and Grant MacGregor (University of California Irvine) for suggestions to the manuscript.

References

1. Alzheimer’s Association. Alzheimer’s disease facts and figures. *Alzheimer’s Dementia* 2018; 14: 367–429.
2. Janota C, Lemere CA and Brito MA. Dissecting the contribution of vascular alterations and aging to Alzheimer’s disease. *Mol Neurobiol* 2016; 53: 3793–3811.
3. Oddo S, Caccamo A, Shepherd JD, et al. Triple-transgenic model of Alzheimer’s disease with plaques and tangles: intracellular A β and synaptic dysfunction. *Neuron* 2003; 39: 409–421.
4. Alonso AC, Grundke-Iqbal I and Iqbal K. Alzheimer’s disease hyperphosphorylated tau sequesters normal tau into tangles of filaments and disassembles microtubules. *Nat Med* 1996; 2: 783–787.
5. Selkoe DJ. Alzheimer’s disease: genes, proteins, and therapy. *Physiol Rev* 2001; 81: 741–766.
6. Kumar K, Kumar A, Keegan RM, et al. Recent advances in the neurobiology and neuropharmacology of Alzheimer’s disease. *Biomed Pharmacother* 2018; 98: 297–307.
7. Hardy J and Selkoe DJ. The amyloid hypothesis of Alzheimer’s disease: progress and problems on the road to therapeutics. *Science* 2002; 297: 353–356.
8. Lewis J, Dickson DW, Lin W-L, et al. Enhanced neurofibrillary degeneration in transgenic mice expressing mutant tau and APP. *Science* 2001; 293: 1487–1491.
9. Myers A, Holmans P, Marshall H, et al. Susceptibility locus for Alzheimer’s disease on chromosome 10. *Science* 2000; 290: 2304–2305.
10. Van Uden E, Carlson G, George-Hyslop PS, et al. Aberrant presenilin-1 expression downregulates LDL receptor-related protein (LRP): is LRP Central to Alzheimer’s disease pathogenesis? *Mol Cell Neurosci* 1999; 14: 129–140.
11. Terry RD. The pathogenesis of Alzheimer disease: an alternative to the amyloid hypothesis. *J Neuropathol Exp Neurol* 1996; 55: 1023–1025.
12. Braak H, Braak E, Bohl J, et al. Age, neurofibrillary changes, A β -amyloid and the onset of Alzheimer’s disease. *Neurosci Lett* 1996; 210: 87–90.
13. Tolar M, Abushakra S and Sabbagh M. The path forward in Alzheimer’s disease therapeutics: reevaluating the amyloid Cascade hypothesis. *Alzheimer’s Dementia* 2020; 16: 1553–1560.
14. Zlokovic BV. Neurodegeneration and the neurovascular unit. *Nat Med* 2010; 16: 1370–1371.
15. Breteler MMB. Vascular involvement in cognitive decline and dementia: epidemiologic evidence from the Rotterdam study and the Rotterdam scan study. *Ann N Y Acad Sci* 2000; 903: 457–465.
16. de la Torre J, Fortin T, Park G, et al. Chronic cerebrovascular insufficiency induces dementia-like deficits in aged rats. *Brain Res* 1992; 582: 186–195.
17. Guariglia CC. Spatial working memory in Alzheimer’s disease: a study using the Corsi block-tapping test. *Dement Neuropsychol* 2007; 1: 392–395.
18. Faden AI and Loane DJ. Chronic neurodegeneration after traumatic brain injury: Alzheimer disease, chronic traumatic encephalopathy, or persistent neuroinflammation? *Neurotherapeutics* 2015; 12: 143–150.
19. Johnson VE, Stewart W and Smith DH. Traumatic brain injury and amyloid- β pathology: a link to Alzheimer’s disease? *Nat Rev Neurosci* 2010; 11: 361–370.
20. Ikonovic MD, Uryu K, Abrahamson EE, et al. Alzheimer’s pathology in human temporal cortex surgically excised after severe brain injury. *Exp Neurol* 2004; 190: 192–203.
21. Roberts G, Gentleman S, Lynch A, et al. Beta amyloid protein deposition in the brain after severe head

- injury: implications for the pathogenesis of Alzheimer's disease. *J Neurol Neurosurg Psychiatry* 1994; 57: 419–425.
22. Nation DA, Sweeney MD, Montagne A, et al. Blood–brain barrier breakdown is an early biomarker of human cognitive dysfunction. *Nat Med* 2019; 25: 270–276.
 23. Viticchi G, Falsetti L, Vernieri F, et al. Vascular predictors of cognitive decline in patients with mild cognitive impairment. *Neurobiol Aging* 2012; 33: e1127–e1129.
 24. Do TM, Alata W, Dodacki A, et al. Altered cerebral vascular volumes and solute transport at the blood–brain barriers of two transgenic mouse models of Alzheimer's disease. *Neuropharmacology* 2014; 81: 311–317.
 25. Nelson AR, Sweeney MD, Sagare AP, et al. Neurovascular dysfunction and neurodegeneration in dementia and Alzheimer's disease. *Biochim Biophys Acta* 2016; 1862: 887–900.
 26. Yamada M and Naiki H. Cerebral amyloid angiopathy. In: David B. Teplow (Ed.), *Progress in molecular biology and translational science*. Elsevier, 2012, pp.41–78.
 27. Thal DR, Ghebremedhin E, Rüb U, et al. Two types of sporadic cerebral amyloid angiopathy. *J Neuropathol Exp Neurol* 2002; 61: 282–293.
 28. Domnitz SB, Robbins EM, Hoang AW, et al. Progression of cerebral amyloid angiopathy in transgenic mouse models of Alzheimer disease. *J Neuropathol Exp Neurol* 2005; 64: 588–594.
 29. Robbins EM, Betensky RA, Domnitz SB, et al. Kinetics of cerebral amyloid angiopathy progression in a transgenic mouse model of Alzheimer disease. *J Neurosci* 2006; 26: 365–371.
 30. Dorr A, Sahota B, Chinta LV, et al. Amyloid- β -dependent compromise of microvascular structure and function in a model of Alzheimer's disease. *Brain* 2012; 135: 3039–3050.
 31. Roher AE, Lowenson JD, Clarke S, et al. beta-Amyloid-(1-42) is a major component of cerebrovascular amyloid deposits: implications for the pathology of Alzheimer disease. *Proc Natl Acad Sci U S A* 1993; 90: 10836–10840.
 32. Yamada M. Risk factors for cerebral amyloid angiopathy in the elderly. *Ann NY Acad Sci* 2002; 977: 37–44.
 33. Götz J, Bodea L-G and Goedert M. Rodent models for Alzheimer disease. *Nat Rev Neurosci* 2018; 19: 583–598.
 34. Kitazawa M, Medeiros RM and LaFerla F. Transgenic mouse models of Alzheimer disease: developing a better model as a tool for therapeutic interventions. *Curr Pharm Des* 2012; 18: 1131–1147.
 35. Games D, Adams D, Alessandrini R, et al. Alzheimer-type neuropathology in transgenic mice overexpressing V717F β -amyloid precursor protein. *Nature* 1995; 373: 523–527.
 36. Zago W, Schroeter S, Guido T, et al. Vascular alterations in PDAPP mice after anti-A β immunotherapy: implications for amyloid-related imaging abnormalities. *Alzheimers Dement* 2013; 9: S105–S115.
 37. Hsiao K, Chapman P, Nilsen S, et al. Correlative memory deficits, A β elevation, and amyloid plaques in transgenic mice. *Science* 1996; 274: 99–103.
 38. Paris D, Patel N, DelleDonne A, et al. Impaired angiogenesis in a transgenic mouse model of cerebral amyloidosis. *Neurosci Lett* 2004; 366: 80–85.
 39. Zhang Y, Chao F, Zhang L, et al. Quantitative study of the capillaries within the white matter of the Tg2576 mouse model of Alzheimer's disease. *Brain Behav* 2019; 9: e01268.
 40. Shin HK, Jones PB, Garcia-Alloza M, et al. Age-dependent cerebrovascular dysfunction in a transgenic mouse model of cerebral amyloid angiopathy. *Brain* 2007; 130: 2310–2319.
 41. Ayata C, Shin HK, Salomone S, et al. Pronounced hypoperfusion during spreading depression in mouse cortex. *J Cereb Blood Flow Metab* 2004; 24: 1172–1182.
 42. Sturchler-Pierrat C, Abramowski D, Duke M, et al. Two amyloid precursor protein transgenic mouse models with Alzheimer disease-like pathology. *Proc Natl Acad Sci U S A* 1997; 94: 13287–13292.
 43. Kelly P, Bondolfi L, Hunziker D, et al. Progressive age-related impairment of cognitive behavior in AP. P23 Transgenic mice. *Neurobiol Aging* 2003; 24: 365–378.
 44. Krucker T, Lang A and Meyer EP. New polyurethane-based material for vascular corrosion casting with improved physical and imaging characteristics. *Microsc Res Tech* 2006; 69: 138–147.
 45. Beckmann N, Schuler A, Mueggler T, et al. Age-dependent cerebrovascular abnormalities and blood flow disturbances in APP23 mice modeling alzheimer's disease. *J Neurosci* 2003; 23: 8453–8459.
 46. Meyer EP, Ulmann-Schuler A, Staufenbiel M, et al. Altered morphology and 3D architecture of brain vasculature in a mouse model for alzheimer's disease. *Proc Natl Acad Sci U S A* 2008; 105: 3587–3592.
 47. Krucker T, Schuler A, Meyer EP, et al. Magnetic resonance angiography and vascular corrosion casting as tools in biomedical research: application to transgenic mice modeling Alzheimer's disease. *Neurol Res* 2004; 26: 507–516.
 48. Heinzer S, Krucker T, Stampanoni M, et al. Hierarchical bioimaging and quantification of vasculature in disease models using corrosion casts and micro-computed tomography. In: *Developments in X-ray Tomography IV* 2004. pp.65-76. International Society for Optics and Photonics.
 49. Heinzer S, Krucker T, Stampanoni M, et al. Hierarchical microimaging for multiscale analysis of large vascular networks. *Neuroimage* 2006; 32: 626–636.
 50. Buée L, Hof P, Bouras C, et al. Pathological alterations of the cerebral microvasculature in Alzheimer's disease and related dementing disorders. *Acta Neuropathol* 1994; 87: 469–480.
 51. Buée L, Hof PR and Delacourte A. Brain microvascular changes in Alzheimer's disease and other dementias a. *Ann N Y Acad Sci* 1997; 826: 7–24.
 52. Fischer V, Siddiqi A and Yusufaly Y. Altered angioarchitecture in selected areas of brains with

- Alzheimer's disease. *Acta Neuropathol* 1990; 79: 672–679.
53. Heinzer S, Krucker T, Meyerc EP, et al. Hierarchical assessment of vascular alterations in a mouse model for Alzheimer's disease. In: *3rd IEEE international symposium on biomedical imaging: nano to macro*. Piscataway, NJ: IEEE, 2006, pp.149–152.
 54. Grothe MJ, Barthel H, Sepulcre J, Alzheimer's Disease Neuroimaging Initiative, et al. In vivo staging of regional amyloid deposition. *Neurology* 2017; 89: 2031–2038.
 55. Palmqvist S, Schöll M, Strandberg O, et al. Earliest accumulation of β -amyloid occurs within the default-mode network and concurrently affects brain connectivity. *Nat Commun* 2017; 8: 1214.
 56. Borchelt DR, Ratovitski T, Van Lare J, et al. Accelerated amyloid deposition in the brains of transgenic mice coexpressing mutant presenilin 1 and amyloid precursor proteins. *Neuron* 1997; 19: 939–945.
 57. Kelly P, Denver P, Satchell SC, et al. Microvascular ultrastructural changes precede cognitive impairment in the murine APP^{swe}/PS1^{dE9} model of Alzheimer's disease. *Angiogenesis* 2017; 20: 567–580.
 58. Kelly P, McClean PL, Ackermann M, et al. Restoration of cerebral and systemic microvascular architecture in APP/PS 1 transgenic mice following treatment with liraglutideTM. *Microcirculation* 2015; 22: 133–145.
 59. Zhang X, Yin X, Zhang J, et al. High-resolution mapping of brain vasculature and its impairment in the hippocampus of Alzheimer's disease mice. *Natl Sci Rev* 2019; 6: 1223–1238.
 60. Lee GD, Aruna JH, Barrett PM, et al. Stereological analysis of microvascular parameters in a double transgenic model of Alzheimer's disease. *Brain Res Bull* 2005; 65: 317–322.
 61. Ciuricǎ S, Lopez-Sublet M, Loeys BL, et al. Arterial tortuosity: novel implications for an old phenotype. *Hypertension* 2019; 73: 951–960.
 62. Wang Y, Liu J, Zhang Z, et al. Structure and permeability changes of the blood-brain barrier in APP/PS1 mice: an Alzheimer's disease animal model. *Neurochem J* 2011; 5: 220–222.
 63. Minogue AM, Jones RS, Kelly RJ, et al. Age-associated dysregulation of microglial activation is coupled with enhanced blood-brain barrier permeability and pathology in APP/PS1 mice. *Neurobiol Aging* 2014; 35: 1442–1452.
 64. Poduslo JF, Curran GL, Wengenack TM, et al. Permeability of proteins at the blood–brain barrier in the normal adult mouse and double transgenic mouse model of Alzheimer's disease. *Neurobiol Dis* 2001; 8: 555–567.
 65. Bennett RE, Robbins AB, Hu M, et al. Tau induces blood vessel abnormalities and angiogenesis-related gene expression in P301L transgenic mice and human Alzheimer's disease. *Proc Natl Acad Sci U S A* 2018; 115: E1289–E1298.
 66. Sadleir KR, Eimer WA, Cole SL, et al. $A\beta$ reduction in BACE1 heterozygous null 5xFAD mice is associated with transgenic APP level. *Mol Neurodegener* 2015; 10: 1.
 67. Oakley H, Cole SL, Logan S, et al. Intraneuronal β -amyloid aggregates, neurodegeneration, and neuron loss in transgenic mice with five familial Alzheimer's disease mutations: potential factors in amyloid plaque formation. *J Neurosci* 2006; 26: 10129–10140.
 68. Giannoni P, Arango-Lievano M, Neves ID, et al. Cerebrovascular pathology during the progression of experimental Alzheimer's disease. *Neurobiol Dis* 2016; 88: 107–117.
 69. Ahn K-C, Learman CR, Dunbar GL, et al. Characterization of impaired cerebrovascular structure in APP/PS1 mouse brains. *Neuroscience* 2018; 385: 246–254.
 70. Kook S-Y, Hong HS, Moon M, et al. $A\beta$ 1–42-RAGE interaction disrupts tight junctions of the blood–brain barrier via Ca²⁺-calcineurin signaling. *J Neurosci* 2012; 32: 8845–8854.
 71. Xu W, Xu F, Anderson ME, et al. Cerebral microvascular rather than parenchymal amyloid- β protein pathology promotes early cognitive impairment in transgenic mice. *J Alzheimers Dis* 2014; 38: 621–632.
 72. Bussière T, Bard F, Barbour R, et al. Morphological characterization of thioflavin-S-positive amyloid plaques in transgenic Alzheimer mice and effect of passive $A\beta$ immunotherapy on their clearance. *Am J Pathol* 2004; 165: 987–995.
 73. Smith AJ, Duan T and Verkman AS. Aquaporin-4 reduces neuropathology in a mouse model of Alzheimer's disease by remodeling peri-plaque astrocyte structure. *Acta Neuropathol Commun* 2019; 7: 74.
 74. Chishti MA, Yang D-S, Janus C, et al. Early-onset amyloid deposition and cognitive deficits in transgenic mice expressing a double mutant form of amyloid precursor protein 695. *J Biol Chem* 2001; 276: 21562–21570.
 75. Weller RO, Preston SD, Subash M, et al. Cerebral amyloid angiopathy in the aetiology and immunotherapy of Alzheimer disease. *Alzheimers Res Ther* 2009; 1: 6.
 76. Lai AY, Dorr A, Thomason LA, et al. Venular degeneration leads to vascular dysfunction in a transgenic model of Alzheimer's disease. *Brain* 2015; 138: 1046–1058.
 77. Davis J, Xu F, Deane R, et al. Early-onset and robust cerebral microvascular accumulation of amyloid β -protein in transgenic mice expressing low levels of a vasculotropic dutch/Iowa mutant form of amyloid β -protein precursor. *J Biol Chem* 2004; 279: 20296–20306.
 78. Herzog MC, Winkler DT, Burgermeister P, et al. $A\beta$ is targeted to the vasculature in a mouse model of hereditary cerebral hemorrhage with amyloidosis. *Nat Neurosci* 2004; 7: 954–960.
 79. Herzog MC, Paganetti P, Staufenbiel M, et al. BACE1 and mutated presenilin-1 differently modulate $A\beta$ 40 and $A\beta$ 42 levels and cerebral amyloidosis in APP^{Dutch} transgenic mice. *Neurodegener Dis* 2007; 4: 127–135.
 80. Herzog MC, Eisele YS, Staufenbiel M, et al. E22Q-mutant $A\beta$ peptide ($A\beta$ ^{Dutch}) increases vascular but reduces parenchymal $A\beta$ deposition. *Am J Pathol* 2009; 174: 722–726.

81. Herzig MC, Van Nostrand WE and Jucker M. Mechanism of cerebral β -amyloid angiopathy: murine and cellular models. *Brain Pathol* 2006; 16: 40–54.
82. De Jonghe C, Esselens C, Kumar-Singh S, et al. Pathogenic APP mutations near the γ -secretase cleavage site differentially affect $A\beta$ secretion and APP C-terminal fragment stability. *Hum Mol Genet* 2001; 10: 1665–1671.
83. Theuns J, Marjaux E, Vandenbulcke M, et al. Alzheimer dementia caused by a novel mutation located in the APP C-terminal intracytosolic fragment. *Hum Mutat* 2006; 27: 888–896.
84. Goate A, Chartier-Harlin M-C, Mullan M, et al. Segregation of a missense mutation in the amyloid precursor protein gene with familial Alzheimer's disease. *Nature* 1991; 349: 704–706.
85. Van Dorpe J, Smeijers L, Dewachter I, et al. Prominent cerebral amyloid angiopathy in transgenic mice overexpressing the London mutant of human APP in neurons. *Am J Pathol* 2000; 157: 1283–1298.
86. Bourasset F, Ouellet M, Tremblay C, et al. Reduction of the cerebrovascular volume in a transgenic mouse model of Alzheimer's disease. *Neuropharmacology* 2009; 56: 808–813.
87. Altman R and Rutledge JC. The vascular contribution to Alzheimer's disease. *Clin Sci (Lond)* 2010; 119: 407–421.
88. Bell RD and Zlokovic BV. Neurovascular mechanisms and blood–brain barrier disorder in Alzheimer's disease. *Acta Neuropathol* 2009; 118: 103–113.
89. Farrall AJ and Wardlaw JM. Blood–brain barrier: ageing and microvascular disease – systematic review and Meta-analysis. *Neurobiol Aging* 2009; 30: 337–352.
90. Donahue JE, Flaherty SL, Johanson CE, et al. RAGE, LRP-1, and amyloid-beta protein in Alzheimer's disease. *Acta Neuropathol* 2006; 112: 405–415.
91. Shinohara M, Tachibana M, Kanekiyo T, et al. Role of LRP1 in the pathogenesis of Alzheimer's disease: evidence from clinical and preclinical studies. *J Lipid Res* 2017; 58: 1267–1281.
92. Miller MC, Tavares R, Johanson CE, et al. Hippocampal RAGE immunoreactivity in early and advanced Alzheimer's disease. *Brain Res* 2008; 1230: 273–280.
93. Yan SD, Chen X, Fu J, et al. RAGE and amyloid- β peptide neurotoxicity in Alzheimer's disease. *Nature* 1996; 382: 685–691.
94. Deane R, Du Yan S, Subramanian RK, et al. RAGE mediates amyloid- β peptide transport across the blood–brain barrier and accumulation in brain. *Nat Med* 2003; 9: 907–913.
95. Zhang WW, Badonic T, Höög A, et al. Astrocytes in Alzheimer's disease express immunoreactivity to the vaso-constrictor endothelin-1. *J Neurol Sci* 1994; 122: 90–96.
96. Jiang MH, Höög A, Ma K-C, et al. Endothelin-1-like immunoreactivity is expressed in human reactive astrocytes. *Neuroreport* 1993; 4: 935–937.
97. Kanekiyo T, Liu C-C, Shinohara M, et al. LRP1 in brain vascular smooth muscle cells mediates local clearance of Alzheimer's amyloid- β . *J Neurosci* 2012; 32: 16458–16465.
98. Jaeger LB, Dohgu S, Hwang MC, et al. Testing the neurovascular hypothesis of Alzheimer's disease: LRP-1 antisense reduces blood–brain barrier clearance, increases brain levels of amyloid- β protein, and impairs cognition. *J Alzheimers Dis* 2009; 17: 553–570.
99. Nelson AR, Sagare AP and Zlokovic BV. Role of clusterin in the brain vascular clearance of amyloid- β . *Proc Natl Acad Sci U S A* 2017; 114: 8681–8682.
100. Hawkes CA, Jayakody N, Johnston DA, et al. Failure of perivascular drainage of β -amyloid in cerebral amyloid angiopathy. *Brain Pathol* 2014; 24: 396–403.
101. Carare R, Bernardes-Silva M, Newman T, et al. Solutes, but not cells, drain from the brain parenchyma along basement membranes of capillaries and arteries: significance for cerebral amyloid angiopathy and neuroimmunology. *Neuropathol Appl Neurobiol* 2008; 34: 131–144.
102. Hawkes CA, Härtig W, Kacza J, et al. Perivascular drainage of solutes is impaired in the ageing mouse brain and in the presence of cerebral amyloid angiopathy. *Acta Neuropathol* 2011; 121: 431–443.
103. Da Mesquita S, Louveau A, Vaccari A, et al. Functional aspects of meningeal lymphatics in ageing and Alzheimer's disease. *Nature* 2018; 560: 185–191.
104. Hawkes CA, Gatherer M, Sharp MM, et al. Regional differences in the morphological and functional effects of aging on cerebral basement membranes and perivascular drainage of amyloid- β from the mouse brain. *Aging Cell* 2013; 12: 224–236.
105. Kouznetsova E, Klingner M, Sorger D, et al. Developmental and amyloid plaque-related changes in cerebral cortical capillaries in transgenic Tg2576 Alzheimer mice. *Int J Dev Neurosci* 2006; 24: 187–193.
106. Hooijmans CR, Graven C, Dederen PJ, et al. Amyloid beta deposition is related to decreased glucose transporter-1 levels and hippocampal atrophy in brains of aged APP/PS1 mice. *Brain Res* 2007; 1181: 93–103.
107. Rasmussen MK, Mestre H and Nedergaard M. The glymphatic pathway in neurological disorders. *Lancet Neurol* 2018; 17: 1016–1024.
108. Asgari M, De Zélicourt D and Kurtcuoglu V. Glymphatic solute transport does not require bulk flow. *Sci Rep* 2016; 6: 38635.
109. Holter KE, Kehlet B, Devor A, et al. Interstitial solute transport in 3D reconstructed neuropil occurs by diffusion rather than bulk flow. *Proc Natl Acad Sci U S A* 2017; 114: 9894–9899.
110. Smith AJ, Yao X, Dix JA, et al. Test of the 'glymphatic' hypothesis demonstrates diffusive and aquaporin-4-independent solute transport in rodent brain parenchyma. *Elife* 2017; 6: e27679.
111. Zhang JH, Badaut J, Tang J, et al. The vascular neural network—a new paradigm in stroke pathophysiology. *Nat Rev Neurol* 2012; 8: 711–716.
112. Hawkins BT and Davis TP. The blood–brain barrier/neurovascular unit in health and disease. *Pharmacol Rev* 2005; 57: 173–185.

113. Higuchi Y, Miyakawa T, Shimoji A, et al. Ultrastructural changes of blood vessels in the cerebral cortex in Alzheimer's disease. *Jpn J Psychiatry Neurol* 1987; 41: 283–290.
114. Kawai M, Kalara RN, Cras P, et al. Degeneration of vascular muscle cells in cerebral amyloid angiopathy of Alzheimer disease. *Brain Res* 1993; 623: 142–146.
115. Davis-Salinas J, Saporito-Irwin SM, Cotman CW, et al. Protein induces its own production in cultured degenerating cerebrovascular smooth muscle cells. *J Neurochem* 1995; 65: 931–934. Amyloid β
116. Yin X, Wright J, Wall T, et al. Brain endothelial cells synthesize neurotoxic thrombin in Alzheimer's disease. *Am J Pathol* 2010; 176: 1600–1606.
117. Ciallella JR, Figueiredo H, Smith-Swintosky V, et al. Thrombin induces surface and intracellular secretion of amyloid precursor protein from human endothelial cells. *Thromb Haemost* 1999; 81: 630–637.
118. Rodríguez-Arellano J, Parpura V, Zorec R, et al. Astrocytes in physiological aging and Alzheimer's disease. *Neuroscience* 2016; 323: 170–182.
119. Xu Z, Xiao N, Chen Y, et al. Deletion of aquaporin-4 in APP/PS1 mice exacerbates brain A β accumulation and memory deficits. *Mol Neurodegener* 2015; 10: 58.
120. Yang W, Wu Q, Yuan C, et al. Aquaporin-4 mediates astrocyte response to β -amyloid. *Mol Cell Neurosci* 2012; 49: 406–414.
121. Wilcock DM, Vitek MP and Colton CA. Vascular amyloid alters astrocytic water and potassium channels in mouse models and humans with Alzheimer's disease. *Neuroscience* 2009; 159: 1055–1069.
122. Yang J, Lunde LK, Nuntagij P, et al. Loss of astrocyte polarization in the tg-ArcSwe mouse model of Alzheimer's disease. *J Alzheimers Dis* 2011; 27: 711–722.
123. Zeppenfeld DM, Simon M, Haswell JD, et al. Association of perivascular localization of aquaporin-4 with cognition and Alzheimer disease in aging brains. *JAMA Neurol* 2017; 74: 91–99.
124. Wolburg H, Noell S, Wolburg-Buchholz K, et al. Agrin, aquaporin-4, and astrocyte polarity as an important feature of the blood-brain barrier. *Neuroscientist* 2009; 15: 180–193.
125. Zhou J, Kong H, Hua X, et al. Altered blood-brain barrier integrity in adult aquaporin-4 knockout mice. *Neuroreport* 2008; 19: 1–5.
126. Winkler EA, Sagare AP and Zlokovic BV. The pericyte: a forgotten cell type with important implications for Alzheimer's disease? *Brain Pathol* 2014; 24: 371–386.
127. Nortley R, Korte N, Izquierdo P, et al. Amyloid β oligomers constrict human capillaries in Alzheimer's disease via signaling to pericytes. *Science* 2019; 365: eaav9518.
128. Brown WR. A review of string vessels or collapsed, empty basement membrane tubes. *J Alzheimer's Dis* 2010; 21: 725–739.
129. Challa VR, Thore CR, Moody DM, et al. Increase of white matter string vessels in Alzheimer's disease. *J Alzheimers Dis* 2004; 6: 379–383.
130. Sagare AP, Bell RD, Zhao Z, et al. Pericyte loss influences Alzheimer-like neurodegeneration in mice. *Nat Commun* 2013; 4: 1–14.
131. Bell RD, Winkler EA, Sagare AP, et al. Pericytes control key neurovascular functions and neuronal phenotype in the adult brain and during brain aging. *Neuron* 2010; 68: 409–427.
132. Mhatre M, Nguyen A, Kashani S, et al. Thrombin, a mediator of neurotoxicity and memory impairment. *Neurobiol Aging* 2004; 25: 783–793.
133. Chen B, Cheng Q, Yang K, et al. Thrombin mediates severe neurovascular injury during ischemia. *Stroke* 2010; 41: 2348–2352.
134. Kantarci K, Gunter JL, Tosakulwong N, Alzheimer's Disease Neuroimaging Initiative, et al. Focal hemosiderin deposits and β -amyloid load in the ADNI cohort. *Alzheimer's Dementia* 2013; 9: S116–S123.
135. Lahiri DK, Farlow MR, Greig NH, et al. Current drug targets for Alzheimer's disease treatment. *Drug Dev Res* 2002; 56: 267–281.
136. Nauck M. Incretin therapies: highlighting common features and differences in the modes of action of glucagon-like peptide-1 receptor agonists and dipeptidyl peptidase-4 inhibitors. *Diabetes Obes Metab* 2016; 18: 203–216.
137. Kastin AJ, Akerstrom V and Pan W. Interactions of glucagon-like peptide-1 (GLP-1) with the blood-brain barrier. *J Mol Neurosci* 2002; 18: 7–14.
138. Perry T, Holloway HW, Weerasuriya A, et al. Evidence of GLP-1-mediated neuroprotection in an animal model of pyridoxine-induced peripheral sensory neuropathy. *Exp Neurol* 2007; 203: 293–301.
139. Jefferies WA, Brandon MR, Hunt SV, et al. Transferrin receptor on endothelium of brain capillaries. *Nature* 1984; 312: 162–163.
140. De Domenico I, Ward DM and Kaplan J. Regulation of iron acquisition and storage: consequences for iron-linked disorders. *Nat Rev Mol Cell Biol* 2008; 9: 72–81.
141. van Duijn S, Bulk M, van Duinen SG, et al. Cortical iron reflects severity of Alzheimer's disease. *Jad* 2017; 60: 1533–1545.
142. Bourassa P, Alata W, Tremblay C, et al. Transferrin receptor-mediated uptake at the blood-brain barrier is not impaired by Alzheimer's disease neuropathology. *Mol Pharm* 2019; 16: 583–594.
143. Paris-Robidas S, Emond V, Tremblay C, et al. In vivo labeling of brain capillary endothelial cells after intravenous injection of monoclonal antibodies targeting the transferrin receptor. *Mol Pharmacol* 2011; 80: 32–39.
144. Cabezón I, Augé E, Bosch M, et al. Serial block-face scanning electron microscopy applied to study the trafficking of 8D3-coated gold nanoparticles at the blood-brain barrier. *Histochem Cell Biol* 2017; 148: 3–12.
145. Loureiro JA, Gomes B, Fricker G, et al. Cellular uptake of PLGA nanoparticles targeted with anti-amyloid and anti-transferrin receptor antibodies for Alzheimer's disease treatment. *Colloids Surf B Biointerfaces* 2016; 145: 8–13.

146. Soto C, Kindy MS, Baumann M, et al. Inhibition of Alzheimer's amyloidosis by peptides that prevent β -sheet conformation. *Biochem Biophys Res Commun* 1996; 226: 672–680.
147. Bien-Ly N, Boswell CA, Jeet S, et al. Lack of widespread BBB disruption in Alzheimer's disease models: focus on therapeutic antibodies. *Neuron* 2015; 88: 289–297.
148. Morrone CD, Bishay J and McLaurin J. Potential role of venular amyloid in Alzheimer's disease pathogenesis. *IJMS* 2020; 21: 1985.
149. Onos KD, Uyar A, Keezer KJ, et al. Enhancing face validity of mouse models of Alzheimer's disease with natural genetic variation. *PLoS Genet* 2019; 15: e1008155.